Effective Parameters for Helical Pole Climbing of the Wheel-based Modular Snake Robot

Pongsakorn Polchankajorn and Thavida Maneewarn
Institute of FIeld roBOtics (FIBO)
King Mongkut's University of Technology Thonburi
Bangkok, Thailand
dome @ fibo.kmutt.ac.th, praew @ fibo.kmutt.ac.th

Abstract—**This research aims to study the factor that affect pole climbing efficiency of the modular snake robot on the cylindrical pole with constant radius. The wheel-based modular snake is climbing the pole by forming itself into a helical or a spiral shape around the pole and using its driving wheel to propel itself upward along the helical path. The joint configuration of the robot can be found from the relation of helical pitch angle, helical radius, and link length of the robot. Five helical climbing configurations with different helical pitch angles and three spiral climbing configurations with different spiral's end radius were tested on the 18 degree of freedoms, 7 links modular hyper-redundant robot. The experimental result showed that the climbing velocity depends on the distribution of the grasping force and the helical pitch angle. The grasping force is affected by the helical radius and the helical pitch angle.**

Keywords-Modular Snake Robot; Helical climbing; Spiral climbing; Pole climbing

I. INTRODUCTION

Climbing robots have been developed for various applications in the past twenty years. The designs of climbing robot are varied depending on their usages such as pipe inspection, fruit harvesting, wall cleaning etc. The mechanisms for climbing in a robot can be categorized as static and dynamic climbing. In static climbing, grasping and body-extending actions are alternated, for example an inchworm climbing motion suggested in [1, 2]. This type of climbing robot usually has two active grippers and can be used to climb across a branch of pipes or trees. In dynamic climbing, grasping and climbing motions happen simultaneously. This type of climbing results in continuous motion, thus has been applied in pole climbing applications as proposed in [3, 4].

In recent year, the modular and reconfigurable robots have been topic of interest by many groups of robotic researchers [5-9]. With modular design, the robot can adapt itself to perform different tasks in various environments including pole climbing. Choset [7] demonstrated the scenario that a modular robotic snake could successfully grasp and roll up a cylindrical pole. His team also invented the Toroidal Skin Drive (TSD) [8] that could drive the robot up the pole in helical trajectory. Goldman and Hong [9] proposed the cost function analysis for designing and controlling a modular climbing robot. They also applied the helical form for grasping and rolling up the pole.

In this paper, we aim to study the parameters that affect the pole climbing ability of a modular robot in helical configuration. We are also interested in the wheel-based modular snake robot due to the fact that the direction of its wheels can be adjusted to provide some frictional support for the gravitational force that acts on the robot. In helical configuration, there are two parameters that significantly affect the climbing ability i.e. helical radius and helical pitch angle. The helical radius directly affects the grasping force between the robot and the pole. On the other hand, the helical pitch angle relates to the climbing velocity. However, when the helical pitch angle is increasing, the grasping force could be decreasing to the point that the robot may lose its climbing ability. In the next section, we will discuss about the design of climbing gait of the modular wheel-based snake robot. The kinematics of the proposed helical and spiral pole climbing gait will be explained.

The rest of the paper will be organized as follows. Section II describes how the helical pole climbing works, the frame assignments of the robot and the helical and spiral path equations. Section III describes the inverse kinematics and the dynamics equation of the robot. Section IV describes the robot design and the climbing experiments. Finally, the result of experiments will be discussed and concluded in section V and VI.

II. CONCEPT OF POLE CLIMBING

A. Designing pole climbing gait for a modular snake robot

A modular snake robot is designed to be able to perform various types of locomotion such as crawling, rolling and climbing. In order to climb a pole, the robot must apply sufficient grasping force around the pole while moving its body up the pole against the gravitational pull. The helical configuration can be used for this type of motion, because the helical form can provide grasping action while allowing the robot to move upward. For the non-wheel modular snake robot, the robot can roll its body upward when it wraps itself around the pole in a helical configuration [7-9]. For the wheel-based modular snake robot, its wheel can be adjusted to be perpendicular to the ground plane so that the robot can roll its wheel upward vertically as in the non-wheel robot [9]. However, we are interested in the climbing motion that the

This work was supported in part by Junior Science Talent Project, NSTDA.

wheels of the robot are aligned with the helical path and drive the robot upward along the helical path instead of in the vertical direction. This climbing gait has its advantage since the wheel can provide large friction force perpendicular to its rolling direction. This friction force can be partial supports against gravitational force. As long as the grasping force is sufficient, the wheel driving force can be used to drive the robot upward with less amount of force compared to the climbing gait with vertical driven wheels or rolling body.

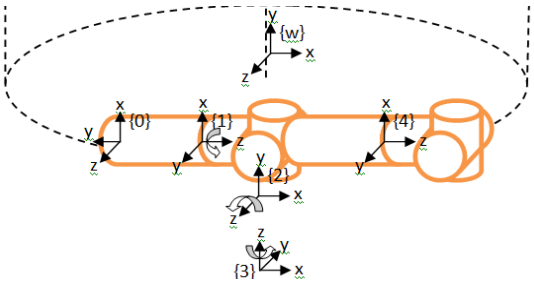

Figure 1. Robot's frame assignment.

With this helical climbing gait, all wheels of the robot must be in contact with the pole surface. In our design, each robot module consists of three revolute joints that can rotate around x, y and z axis. The wheel axis in each module is aligned with the x axis of the 4th frame. *W* and *n* designate the world frame and number of modules. The frame reference for each module can be described by the transformation matrix ${}^{W}_{4}T$. The transformation equation of the robot with n modules can be written as follow.

$$ {}^{W}_{n}T = \left({}^{W}_{4}T\right)_1 \cdot \left({}^{0}_{4}T\right)_2 \cdots\cdots \left({}^{0}_{4}T\right)_n \tag{1} $$

B. *Circular helical and spiral path*

The circular helical path is the three dimensional helix with a constant radius. We can use 3 equations to describe a three dimensional helical path as follow.

$$ x(s) = R\cos(s) \tag{2} $$

$$ y(s) = bs \tag{3} $$

$$ z(s) = R\sin(s) \tag{4} $$

Where R is the helical path radius on xz plane (top view) and $2\pi b$ is the helical pitch angle. We can change helix path to spiral path by changing the R constant to a function that varied by the height of the spiral path (y axis). Example of function R that use in the spiral climbing experiment can be shown as follow. $l, R_{\min}, R_{\max}$ represent the height of overall spiral segment, the minimum and the maximum spiral radius.

$$ R_{Spiral} = \begin{cases} y(s) > \dfrac{l}{2} : R_{\min} + \dfrac{y(s)}{\dfrac{l}{2}} \cdot \left(R_{\max} - R_{\min}\right) \\ y(s) < \dfrac{l}{2} : R_{\max} - \dfrac{y(s) - \dfrac{l}{2}}{\dfrac{l}{2}} \left(R_{\max} - R_{\min}\right) \end{cases} \tag{5} $$

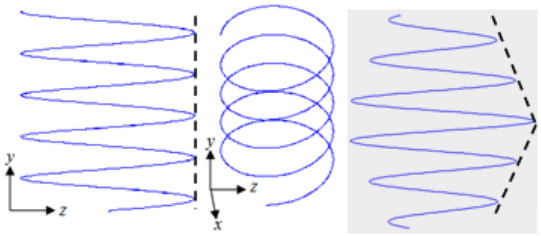

Figure 2. Circular helix path and spiral path.

III. KINEMATICS AND DYNAMICS ANALYSIS

A. *Helical shape approximation*

In order to form a modular snake robot into a helical shape around the pole, the continuous helical and spiral path equations in section II.B has to be discretized according to the robot physical parameters such as type of joints and the length of its link. The helical path can be described by a helical pitch angle and radius. For a given link length (L) of each robot module and with helical radius R , the reference frame of each module can be assigned at the point on the R -radius circle at every θ_{step} angle around y axis as shown in figure 3.

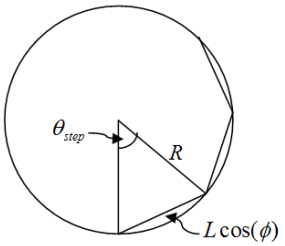

Figure 3. Top view of the helical curve.

For each reference frame, the axis vector x (${}^{w}_{x}P$) and z (${}^{w}_{y}P$) with respect to the world frame can be assigned in the perpendicular and tangential direction of a circular pole surface and along the helical path. The axis vector Y can be found from the cross product of vector of (${}^{w}_{x}P$) and (${}^{w}_{y}P$). Therefore, we can represent the rotation matrix for each module reference frame as follow

$$ {}^{w}_{i}R = \begin{bmatrix} {}^{w}_{x}P & {}^{w}_{y}P & {}^{w}_{z}P \end{bmatrix} \tag{6} $$

Then we can transform the relation of the rotation matrix with respect to the world frame to the rotation matrix i with respect to frame i-1 from the equation.

$$ {}^{i-1}_{i}R = {}^{w}_{i-1}R^{T}\, {}^{w}_{i}R \tag{7} $$

Algebraic method is used to solve for the joint angles of each robot's module by the Euler angle set equation.

$$ \alpha = \text{atan2}(m_{32}, m_{22}) \tag{8} $$

$$ \beta = a\sin(-m_{12}) \tag{9} $$

$$ \gamma = \text{atan2}(m_{13}, m_{11}) \tag{10} $$

B. Dynamic model

The dynamic model of the robot can be derived from Lagrangian method assuming that the contact of all robot's wheels and the pole are under non-slipped condition. The general form of the link's equation can be written as follow.

$$\tau_i = M_i(q_i)\ddot{q}_i + V_i(q_i,\dot{q}_i) + G_i(q_i) + J_i(q_i)\lambda \quad (11)$$

With $q_i = \begin{bmatrix}\alpha_i & \beta_i & \gamma_i & \theta_i\end{bmatrix}^T$ and $\tau_i = \begin{bmatrix}\tau_{\alpha_i} & \tau_{\beta_i} & \tau_{\gamma_i} & \tau_{\theta_i}\end{bmatrix}^T$.

Assume i as the number of link.

The angles α_i, β_i, γ_i, θ_i, τ_{α_i}, τ_{β_i}, τ_{γ_i}, and τ_{θ_i} are the roll angle, pitch angle, yaw angle, rolling angle of robot's wheel, roll torque, pitch torque, yaw torque, and wheel's torque, respectively. $J_i(q_i)\lambda$ is the non-holonomic constraint term that has the null space of linear-velocity transform.

$$J_i^T(q_i)\dot{q} = 0 \quad (12)$$

From the local matrix, each module of the robot has four control parameters and joint variables and one non- holonomic constraint. Therefore, the robot that consists of *n* modules would have *4n* control parameters and joint variables. The total number of non-holonomic constraints of the robot is *n* constraints. When the robot is formed into the helical configuration, all non-holonomic constraints will align in the direction perpendicular to the helical curve. The spread out view of the pole's surface when the robot is in helical configuration shows that all wheels drive input are perpendicular to the non-holonomic constraints of the wheels, thus satisfies all *n* constraints for the *n*-modules robot.

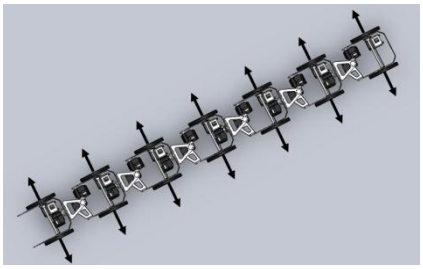

Figure 4. Non-holonomic constraints in the spread out view of the pole surface.

IV. EXPERIMENT

A. Wheel-based modular snake robot system

The robot consists of 7 modules. Each module has 3 revolute actuators (Robotis DX-117) which all axes are intersect. All 3 revolute actuators are positioned controlled. Each module also has two driving wheels. Both wheels are driven by a Robotis RX-28 motor. The robot structure is made of aluminum alloy. The roll joint is supported with superlene nylon to prevent link deflection. The 10-cm diameter wheel is also made from superlene nylon and coated with anti-slip substance. Each module is 19.1 cm long. The total weight of this 7-module robot is approximately 3 kg. Figure 5 shows the complete wheel-based modular snake robot.

Figure 5. The prototype wheel-based modular snake robot.

In order to control the robot, the angular position and the wheel velocity command is sent to the robot from a notebook computer to a microcontroller board on the robot via RS-232. The microcontroller converts these commands into the protocol that is used by the digital servo motor and sends the command packet to all motors via a RS-485 bus. A current sensor is added into each robot module to measure the current for its drive motor. The microcontroller can collect data from the current sensor as well as the load feedback from a digital servo motor. Both data and power are sent to the robot via a 4 meters long cable.

B. Climbing experiment

The experiment was performed to study the relationship between the parameters of the helical climbing path (i.e. the helical pitch angle and the helical radius) and the climbing performance (i.e. climbing velocity and grasping ability).

1) Varying the helical path's pitch angle

This experiment was designed to test the performance of helical climbing at different helical pitch angles. The relationship between the pitch angle, the grasping load, the driving load and the climbing velocity of the robot were focused in this experiment. The test was performed on the wheel-based modular robot which was earlier described in section A. The pole used in this experiment has 14 cm diameter and is covered with carpet. The robot wheel radius is 5 cm. The helical path of 12.75 cm radius was chosen for this experiment (from the calculation in section III.A as shown in fig. 3). According to the robot module dimension and the pole radius, the helical pitch angles were varied at 15, 17.5, 20, 22.5, 25 degree for this experiment. Table I shows the joint angle for each modules at varying helical pitch angle.

TABLE I. JOINT ANGLE USED IN HELICAL CLIMBING EXPERIMENT

Helical pitch angle(degrees)	**15**	**17.5**	**20**	**22.5**	**25**
Roll angle	15.54	18.33	21.15	23.98	26.76
Pitch angle	-15.17	-17.02	-18.57	-19.79	-20.67
Yaw angle	88.62	85.70	82.42	78.82	74.95

During the climbing experiment, data that can indicate the status of the robot was collected e.g. the grasping load, the driving load (i.e. current reading from the drive motor) and the climbing velocity. The climbing tests were performed 5 times

for each helical pitch angle variation. The results are shown in table II, fig. 6, fig. 7, fig.8, and fig. 9.

TABLE II. ABILITY OF HELICAL GRASPING AND CLIMBING IN EACH HELICAL PITCH ANGLE

Helical pitch angle(degrees)	15	17.5	20	22.5	25
Grasping	✓	✓	✓	✓	✓
Climbing	✓	✓	✓	×	×

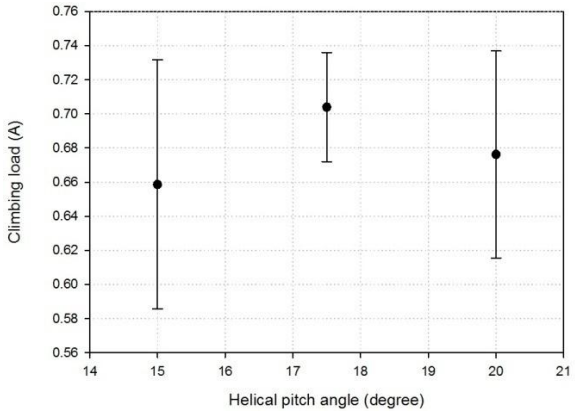

Figure 6. The graph between mean and SD of climbing load and helical pitch angle.

Table II shows that when the helical pitch angle is larger than 20 degrees, the robot can only grasp the pole but cannot climb the pole. When the robot tried to climb the pole under these conditions, the wheel appeared to be slipping and the robot was no longer be able to grasp the pole and slid down eventually.

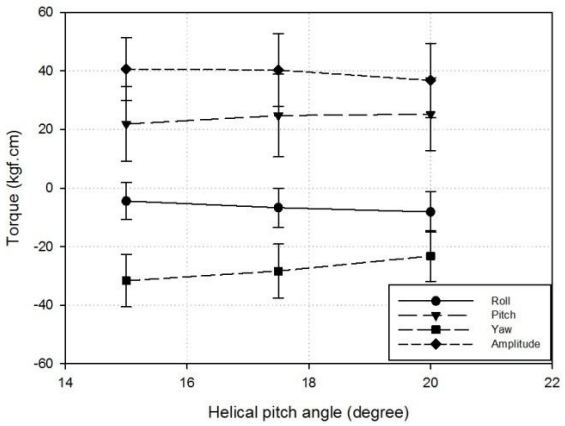

Figure 7. The graph between mean and SD of holding torque in each axis of rotation and helical pitch angle.

2) Varying the path's radius

This experiment was designed to test the climbing performance with different radius profile. From the previous experiment, fig 9 shows that the yaw holding torque for each module were distributed in parabolic form which means that the grasping ability was reduced at each end of the robot (i.e. head and tail).

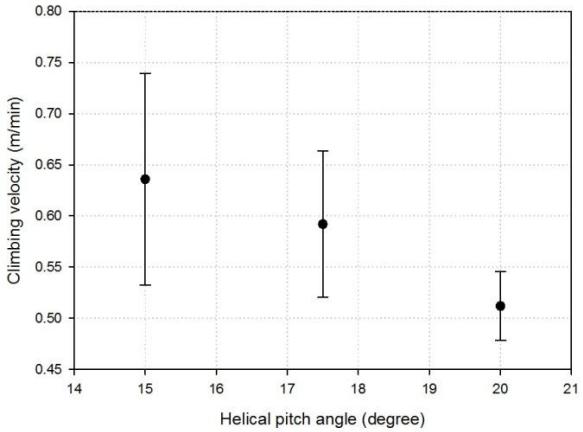

Figure 8. The graph between mean and SD of climbing velocity and helical pitch angle.

The experimental results in figure 8 also showed the inverse relationship between the climbing velocity and the helical pitch angle. Contrary to the kinematic relationship where the higher pitch angle would resulted in more travelling distance over time, the grasping load decrease when the pitch angle increase (as shown in fig. 6) thus caused the climbing ability to drop.

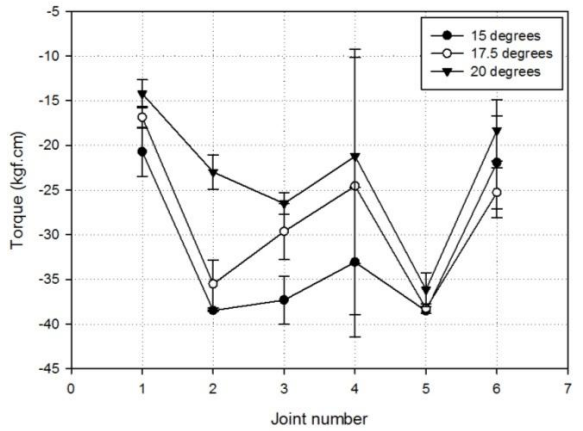

Figure 9. The graph of yaw's torque distribution along the robot's body and the helical pitch angle.

For a helical path, the radius is constant throughout the robot's length. In a spiral path as described in section II, the path's radius is varied along the path. The spiral path is designed to have a smaller path radius at each end to increase the grasping load.

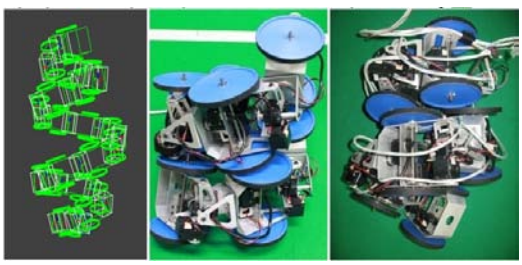

Figure 10. Simulation of spiral pose (left) and the real shape of helical pose (center) and spiral pose (right).

In this experiment, the 15 degrees pitch angle was chosen. The radius of the spiral path at the middle was set to 12.75 cm and both end radiuses were varied at 11, 11.5 and 12 cm due to joint limits of the robot. The climbing test were performed 5 times for each configuration except at the 12-cm case which can be tested only 3 times because the yaw torque at the last module became too high and the motor were no longer be able to hold its position. Results from the experiment are shown in fig. 11-15 and table III.

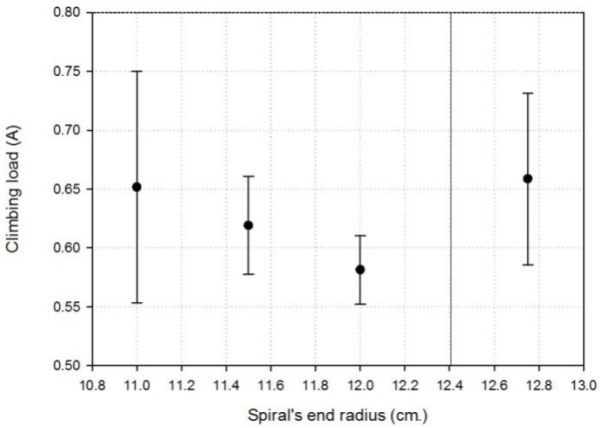

Figure 11. The graph between mean and SD of climbing load of spiral's end radius and helical climbing with 15 degrees pitch angle.

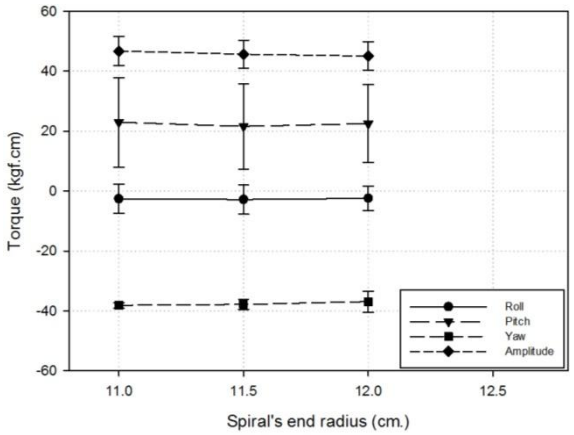

Figure 12. The graph between mean and SD of holding torque in each axis of rotation and spiral's end radius with 15 degrees pitch angle.

Fig. 11 and 12 shows the inverse relationship between the spiral path's end radius and the holding torque of yaw angle. When the spiral end radius decreased, the yaw torque increased which indicated that the grasping ability increased as well. When the grasping ability increased, the robot could hold on to the pole tighter thus resulted in higher climbing velocity. Table III compares the climbing velocity between the helical (fix radius) and the spiral (varying radius) cases. The climbing velocity is higher with the spiral climbing than the helical climbing at the same helical pitch angle.

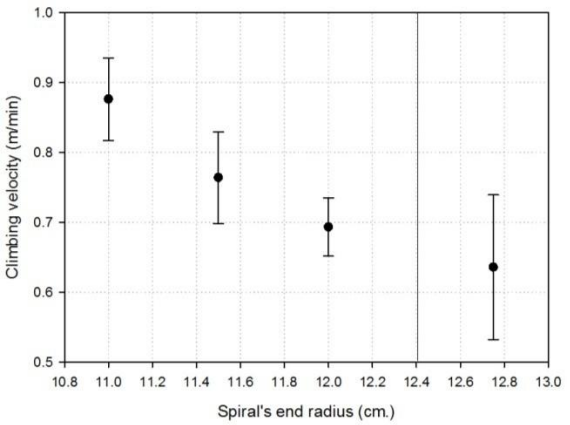

Figure 13. The graph between mean and SD of climbing velocity of spiral's end radius and helical climbing with 15 degrees pitch angle.

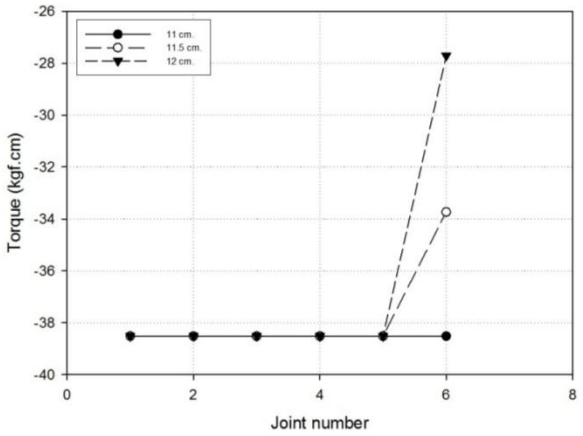

Figure 14. The graph between holding torque of yaw angle and spiral's end radius with 15 degrees pitch angle.

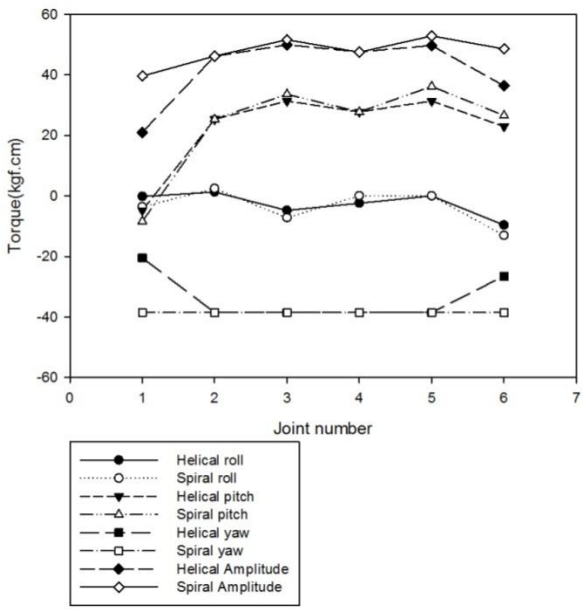

Figure 15. The comparison graph between helical path's holding torque and spiral path's holding torque with 15 degrees pitch angle.

TABLE III. VELOCITY COMPARISON BETWEEN HELICAL AND SPIRAL CLIMBING (M/MIN)

Helical pitch angle(degrees)	Velocity	Spiral radius(cm.)	Velocity
15	0.636	12.75-11	0.876
17.5	0.592	12.75-11.5	0.764
20	0.512	12.75-12	0.693

V. DISCUSSION

From the result of experiments in the previous section, we found that the main contribution that affects the pole climbing performance of the wheel-based modular snake robot is the magnitude and the distribution of force that the robot uses to grasp the pole. Since the robot consisted of n modules, the grasping force distribution directly relates to number of modules, the length of each modules and the pole radius. With the helical (fix radius path) configuration, the grasping load is large at the middle module and small at both ends. When the path radius is too large, the robot cannot produce sufficient amount of grasping force especially at the end modules, thus the robot cannot climb the pole. With the spiral (varying radius) path, the radius of the path are smaller at both ends in order to increase the grasping force at the end modules. The climbing speed can be increase by decreasing the end radius as long as the joint limit and the torque limit of the robot allows.

Another problem that was noticed during the helical climbing experiment is that the wheels of the head module did not always touch the pole surface. We assume that it could be the result of accumulated error from all joints of the robot which can be shown by the Cartesian error that is affected by the joint error from Jacobian relationship in equation 14.

$$\begin{bmatrix} \Delta x \\ \Delta y \\ \Delta z \end{bmatrix} = \begin{bmatrix} J_p \end{bmatrix} \begin{bmatrix} \Delta q_1 \\ \dots \\ \Delta q_{18} \end{bmatrix} \tag{14}$$

The error of each joint was found from the angular reading data during the pole climbing experiment compare with the angle calculated from the helical curve. However, the Cartesian accumulate error ranged from 10 cm to 13 cm, which was much larger than the actual error from our direct observation. The difference may be resulted from the deflection in the rolling joint that occurred in the real robot which was not considered in the kinematic calculation.

VI. CONCLUSION

In this paper, a pole climbing in helical and spiral configuration of the wheel-based modular snake robot was studied. The pole grasping condition was realized by forming the robot into a helical and spiral shape. The wheel-base design is chosen in order to decouple the grasping and climbing action. Wheels are used to propel the robot upward along the pole surface in helical path. All wheel axes need to be parallel to the pole surface which can be realized by performing inverse kinematic calculation from the predefined helix path according to the robot model. Non-slip contact between the robot and the pole can be created by forming the helical path with the sufficiently small radius (according to the pole's radius) and the sufficient static friction coefficient between the wheel and the pole surfaces.

Climbing experiments were performed to study the relationship between different helical path parameters (i.e. pitch angle and radius) and climbing performance (i.e. climbing velocity). With the constant helical path radius, when the helical pitch angle increased, the grasping ability of the robot decreased as shown by the lower grasping force (which is directly related to yaw torque) and the slower climbing velocity. The profile of the yaw torque along the robot's body showed a parabolic relationship which meant that the grasping torque are lower at both end modules than at the middle module. By applying the spiral path which the helical radius are smaller at both ends than in the middle, to compensated the Cartesian error of each joint, the grasping force along the robot's body can be more uniformly distributed. The experiment showed that the spiral climbing can increase the climbing velocity and grasping ability with same actuator's ability. Therefore, main factors that contribute to the pole climbing performance are the magnitude and the distribution of the grasping torque in all robot's modules. According to the kinematic relationship, the higher pitch angle should yield more climbing distance as long as the non-slip contact condition can be maintained. Results from this study can be used for designing a better wheel-based modular snake and modular robot's gait that can climb and crawl in various environments and the inclusion of a force-control scheme into the system in the future.

REFERENCES

[1] Zaidi Mohd. Ripin, Tan Beng Soon, A.B. Abdullah and Zahurin Samad, 2000, "Development of a Low-Cost Modular Pole Climbing Robot", TENCON 2000: 196-200.

[2] M. Almonacid, R. J. Saltarén, R. Aracil, and O. Reinoso, 2003, "Motion Planning of a Climbing Parallel Robot", IEEE Transactions on Robotics and Automation.

[3] Baghani A., Ahmadabadi M.N., Harati A., 2005, "Kinematics Modeling of a Wheel-Based Pole Climbing Robot (UT-PCR)", IEEE International Conference on Robotics and Automation.

[4] W. Chonnaparamutt, H. Kawasaki, S. Ueki, S. Murakami, and K. Koganemaru, 2009, "Development of A Timberjack-like Prunning Robot: Climbing Experiment and Fuzzy Velocity Control", ICROS-SICE International Joint Conference.

[5] H. Kurokawa, K. Tomita, A. Kamimura, S. Murata, Y. Terada, S. Kokaji, 2006, "Distributed Metamorphosis Control of a Modular Robotic System M-TRAN", Distributed Autonomous Robotic Systems (DARS) 7, Springer, 115-124.

[6] Nadeesha Ranasinghe, Jacob Everist, Wei-Min Shen, 2007, "Modular Robot Climber", IEEE/RSJ Intl. Conf. on Intelligent Robots and Systems.

[7] Kevin Lipkin, Isaac Brown, Aaron Peck, Howie Choset, Justine Rembisz, Philip Gianfortoni, Allison Naaktgeboren, 2007. "Differentiable and Piecewise Differentiable Gaits for Snake Robots", IEEE/RSJ International Conference on Intelligent Robots and Systems.

[8] James C. McKenna, David J. Anhalt, Frederick M. Bronson, H. Ben Brown, Michael Schwerin, Elie Shammas, and Howie Choset, 2008. "Toroidal Skin Drive for Snake Robot Locomotion", IEEE International Conference on Robotics and Automation.

[9] G. Goldman and D. W. Hong, 2008, "Considerations for Finding the Optimal Design Parameters for a Novel Pole Climbing Robot", ASME Mechanisms and Robotics Conference.